Mercier Stability Improvement in Nonlinear Development of LHD Plasma

Katsuji ICHIGUCHI[1)] and Benjamin A. CARRERAS[2)]

[1)]*National Institute for Fusion Science, 322-6 Oroshi-cho, Toki 509-5292, Japan*
[2)]*BACV Solutions Inc., 110 Mohawk, Oak Ridge, Tennessee 37831, USA*

(Received / Accepted)

Improvement of linear stability due to the nonlinear saturation of interchange modes in the increase of the beta value is studied for the inward-shifted LHD plasma. For this study, a multi-scale numerical scheme is utilized. In this scheme, the beta value is increased by adding small pressure increment to the background pressure. We focus on the dependence of the Mercier stability on the profiles of the pressure increment. It is obtained that the pressure profile approaches to the marginally stable profile when fixed profiles are employed for the pressure increment.

Keywords: MHD, LHD, multi-scale simulation, Mercier criterion, interchange mode, self-organization

1. Introduction

In the LHD experiments, good confinement of the plasma has been observed in the magnetic configuration with the vacuum magnetic axis located $R_{ax} = 3.6$m[1]. However, linear ideal interchange modes or Mercier modes were predicted to be unstable in this configuration. In order to investigate the stabilizing mechanism of the modes, we developed a nonlinear MHD code, NORM, based on the reduced MHD equations[2, 3]. In such investigation, it is crucial to follow the continuous change of the pressure profile in the increase of the beta value. For this purpose, we have also developed a multi-scale simulation scheme[4] by utilizing the NORM code and the VMEC code[5]. This scheme treats both the equilibrium change in the long time scale and the nonlinear dynamics of the instability in the short time scale simultaneously.

In the multi-scale scheme, the beta value is increased by adding a small increment of pressure to the background pressure obtained as the results of the nonlinear dynamics. In this case, there is a freedom in the determination of the profile of the pressure increment. One choice for the profile is to use the shape similar to the background pressure profile obtained by the nonlinear evolution. In the original study[4], we applied this pressure increment to the inward shifted configuration of LHD. We found a self-organization of the pressure profile which indicated a stable path to high beta regime.

On the other hand, the profiles of the heat deposition and the particle supply in experiments are usually fixed in the increase of beta. In order to take this situation into account, we consider to use a fixed profile for the increment of the pressure in the present study. We employ two types of increment profile and compare the results with that of the similar increment profile. Particularly, we focus on how the Mercier stability is improved by the self-organization of the pressure profile due to the nonlinear saturation of the interchange mode.

2. Multi-scale scheme with fixed pressure increment

The multi-scale scheme used in the present analysis is explained in Ref.[4] precisely. Here we start from a brief review of the multi-scale scheme, and then, explain the choice of the pressure increment profile and the conditions in the calculation.

The scheme consists of iterative calculations of nonlinear dynamics of the perturbations by the NORM code and three-dimensional equilibrium by the VMEC code. In this case, we divide the whole calculation time into short time intervals. At $t = t^i$, the beginning of an interval, we calculate new equilibrium quantities at the higher beta value with the VMEC code as the values of $t = t^{i+1}$, the beginning of the next interval. In order to keep a smooth continuity of the perturbation, we also divide the interval between t^i and t^{i+1} into some sub-intervals and employ a linear interpolation of the equilibrium quantities by using the equilibrium quantities of $t = t^i$ and t^{i+1}. Then, the nonlinear dynamics is calculated for each sub-interval with the interpolated equilibrium quantities with the NORM code.

When we calculate the equilibrium with the VMEC code, we incorporate the pressure deformation due to the nonlinear dynamics into the pressure profile. At $t = t^i$, the total pressure is obtained as

$$P^i_{tot} = \langle P\rangle^i + \sum_{m \neq 0 \text{ or } n \neq 0} \tilde{P}_{mn}, \tag{1}$$

where the tilde means a perturbed quantity and m and n are the poloidal and the toroidal mode numbers. Here $\langle P\rangle^i$ denotes the average pressure which is given by

$$\langle P\rangle^i = P^i_{eq} + \tilde{P}^i_{00}. \tag{2}$$

author's e-mail: ichiguch@nifs.ac.jp

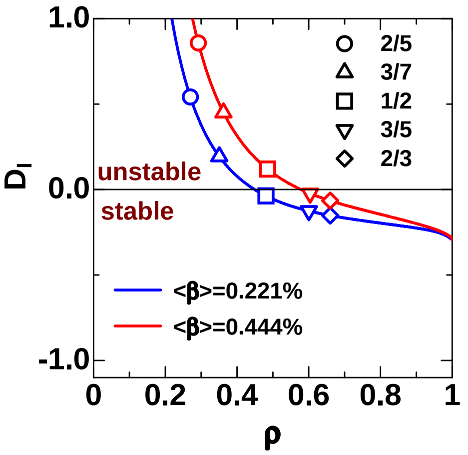

Fig. 1 Profiles of D_I of the equilibrium for the pressure profile of $P_{eq} = P_0(1-\rho^2)(1-\rho^8)$ in the inward-shifted LHD plasma. Each symbol shows the value of D_I at the position of the resonant surface.

The average pressure includes the effect of the nonlinear dynamics through $\tilde{P}^i_{00}$. We calculate P^{i+1}_{eq} by using $\langle P\rangle^i$ as

$$P^{i+1}_{eq} = \langle P\rangle^i + \Delta P^{i+1}. \tag{3}$$

Here ΔP^{i+1} denotes the increment of the pressure, which gives the increase of beta. In the original study[4], we employed a similar increment profile given by

$$\Delta P^{i+1} = \langle P\rangle^i \frac{\beta^{i+1} - \beta^i}{\beta^i}. \tag{4}$$

In the present study, we also consider two kinds of fixed profile for the increment given by

$$\Delta P^{i+1} = P_I(1-\rho^2)(1-\rho^8) \tag{5}$$

and

$$\Delta P^{i+1} = P_I(1-\rho^2)^2, \tag{6}$$

where ρ denotes the square-root of normalized toroidal magnetic flux. The factor P_I is adjusted so as to give a given beta increment. Hereafter, we call the increments given by (4)-(6) 'similar increment', 'parabolic increment' and 'parabola-squared increment', respectively.

We apply the scheme to the LHD plasma for the three types of pressure increment under following numerical conditions. We choose the configuration with the vacuum magnetic axis located at R_{ax} = 3.6m. We assume the resistivity of $S = 10^6$, where S is the magnetic Reynolds number. We examine the evolution for $0.221\% \le \langle\beta\rangle \le 0.498\%$. One time interval is $2500\tau_A$, where τ_A is Alfvén time. We increase the beta value by $\Delta\langle\beta\rangle = 0.0138\%$ every time interval. In the equilibrium calculation with the VMEC code, we use the free boundary condition and the no net-current condition. The time interval is divided into 10 sub-intervals for the linear interpolation.

To give the initial state, we start from the equilibrium for $P_{eq} = P_0(1-\rho^2)(1-\rho^8)$ at $\langle\beta\rangle = 0.221\%$. As is shown

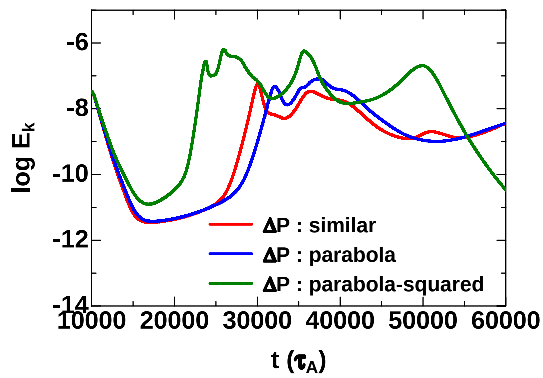

Fig. 2 Time evolution of kinetic energy for each case of the pressure increment.

in Fig.1, the core region of $\rho \le 0.44$ of this equilibrium is Mercier unstable. The absolute value of D_I[6] decreases in the ρ direction. We follow the nonlinear evolution of the interchange mode for this equilibrium and obtain a saturation at $t = 10000\tau_A$. We employ the saturated state as the initial state of the multi-scale calculation and set $t = 10000\tau_A$ as the initial time. Then, the beta value reaches $\langle\beta\rangle = 0.498\%$ at $t = 60000\tau_A$.

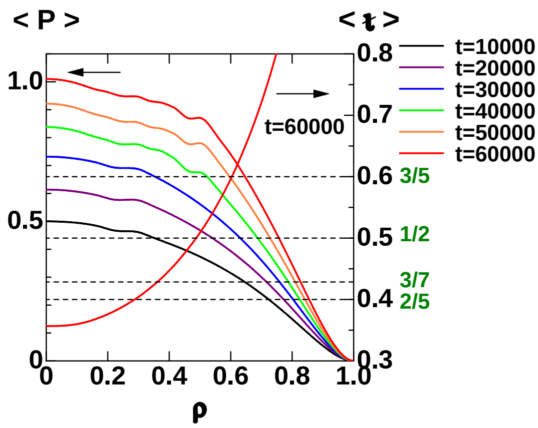

Fig. 3 Time evolution of average pressure in the case of the parabolic increment.

3. Self-organization of pressure profile

We follow the evolution of the plasma for the three types of increment profile and compare the resultant pressure profile. Figure 2 shows the time evolution of the total kinetic energy for the three pressure increments. It is common that the kinetic energy varies smoothly compared with the time scale of sub-interval. This feature indicates the multi-scale approach works well also in the fixed increment cases. The evolution of the parabolic increment case is close to that of the similar increment case, while the evolution in the parabola-squared increment case is a little more active.

Figure 3 shows the time evolution of the average pressure in the case of the parabolic increment. As in the case of the similar increment case[4], weak excitation and mild

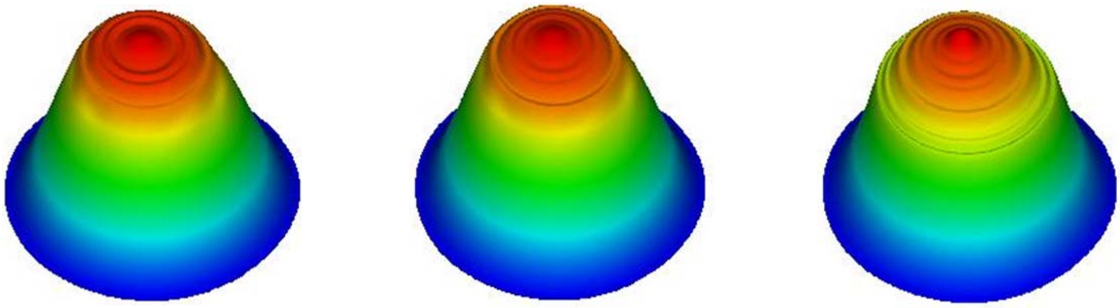

Fig. 4 Bird's-eye view of total pressure at t=60000τ_A for similar increment (left), parabolic increment (center) and parabola-squared increment (right).

saturation of the interchange modes occur. The saturation generates locally flat structure at the resonant surfaces in the average pressure profile. Since the Mercier quantity D_I is a decreasing function of ρ as shown in Fig.1, the flat region is generated from inward to outward of the plasma as the beta increases. Similar tendency is observed in the parabola-squared increment case.

Figure 4 shows the bird's-eye view of the total pressure at the final time of $t = 60000\tau_A$. The deformation of the total pressure is almost θ independent for all increment cases. This implies that almost all of the resonant interchange modes are saturated in a low level without any significant excitation. In other words, in each increment profile, the total plasma pressure evolves so that fluctuations are suppressed in the increase of beta.

Remarkable difference between the three increment profiles is seen in the average pressure profile at the final state. Figure 5 shows the profile of the average pressure at $t = 60000\tau_A$. In the similar increment case, a global flat structure is generated in the core region of $\rho < 0.4$. In the parabolic increment case, the gradient of the pressure is recovered in the core region. In the parabola-squared increment case, the gradient becomes larger. These differences are attributed to the gradient of the increment profile. In any case of the increment, the pressure profile is flattened in the core region once at low beta because (m,n)=(5,2) and (7,3) modes are saturated in the region. In the similar increment case, the average pressure is increased so that the shape should be maintained. Therefore, the local flat structure generated at low beta is kept even at high beta.

On the other hand, in the fixed increment cases, the gradient of the increment profile is always added to the total pressure. Therefore, the local flat structure of the average pressure tends to be smoothed out. Furthermore, the resonant mode can be excited again at the flattened region when the local pressure gradient enhanced by the increment exceeds a critical value. Since the driving force of the mode should be quite weak, it saturates immediately to generate a narrower flat region in the average pressure profile. Thus, the local pressure gradient approaches to the critical value through this process. The critical value can be measured in terms of D_I as explained in the next section.

In the parabolic increment case, the increment profile is the same as the equilibrium profile used in the initial state generation. Therefore, this process is limited in the core region. On the other hand, the more steep gradient is added in the parabola-squared increment case. The region of the process extends to the outer region including the surfaces resonant with the (5,3) and the (3,2) modes.

4. Mercier stability improvement

The global feature of the D_I profile is common in all cases of the increment. Figure 1 (red line) shows the D_I profile for the equilibrium with the pressure profile of $P_{eq} = P_0(1-\rho^2)(1-\rho^8)$ at $\langle\beta\rangle = 0.444\%$. In this case, the wide region of $\rho \leq 0.60$ is Mercier unstable. On the other hand, D_I has negative values around the resonant surfaces as shown in Fig.6, which shows the D_I profiles at $t = 60000\tau_A$ ($\langle\beta\rangle = 0.498\%$) for the three cases of the pressure increment. This comparison shows that the nonlinear saturation of the interchange mode stabilizes itself through the local pressure flattening.

The difference in the structure of the pressure profile is reflected to the precise structure of D_I profile. In the similar increment case, the improved values of D_I are -1.05, -0.49 and -0.21 at resonant surfaces with $\iota = 2/5$, 3/7 and 1/2. There is a tendency that the absolute value is a decreasing function of ρ_s, where ρ_s is the position of the resonant surfaces. This tendency is related to the Mercier stability at the initial equilibrium. The profile of D_I at $\langle\beta\rangle = 0.221\%$ implies that the driving force of the interchange mode is also the decreasing function of ρ. Therefore, the local deformation at inner resonant surface is larger than that at outer surface. Since such structure is almost maintained during the beta increase, the resonant surface is more stabilized beyond the marginal stability.

On the contrary, the absolute value of D_I is limited in the level of -0.32 in the parabolic increment case. In this case, even once the pressure profile is locally flattened, the enhancement of the gradient of the pressure degrades the Mercier stability. Therefore, the value of D_I approaches to a marginal value in the increase of beta. This tendency is the same as in the case of the parabola-squared increment. In this case, the local improvement is observed also

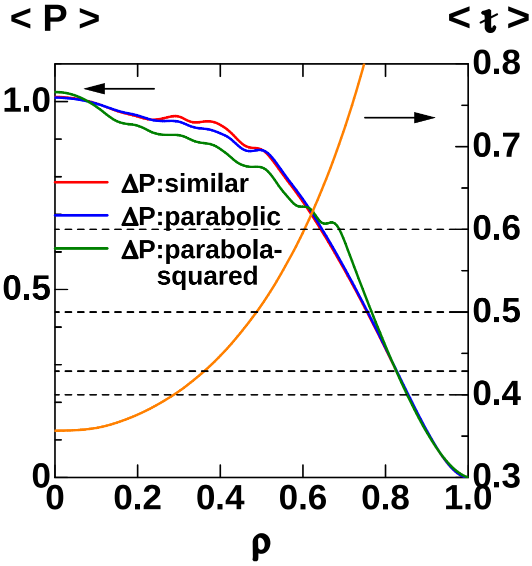

Fig. 5 Average pressure profiles at $t = 60000\tau_A$.

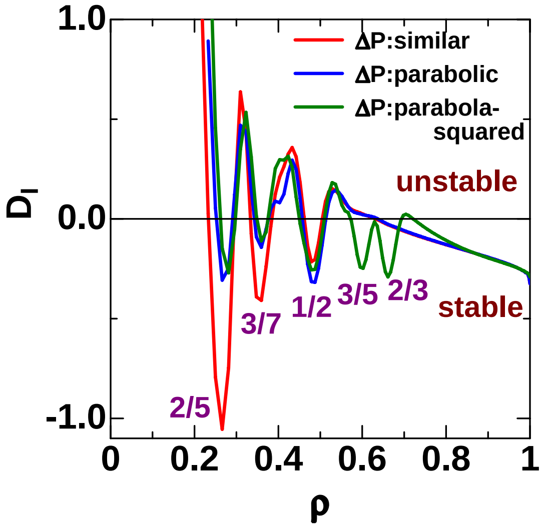

Fig. 6 Profiles of D_I at $t = 60000\tau_A$.

around the surfaces of $\iota = 3/5$ and 2/3. Including these surfaces, the absolute value of D_I is limited in the level of -0.29. The enhancement of the pressure gradient brought by the parabola-squared increment is larger than that by the parabolic increment case. Nevertheless, the maximum value of D_I is in the similar level of $D_I \sim -0.3$. This result indicates that this value of D_I corresponds to the marginal pressure gradient independent of the increment profile, if a fixed increment profile is employed. It can be concluded that the local pressure gradient is determined in the increase of beta so that D_I at the resonant surface should achieve to the marginal value.

5. Conclusions

The local improvement of the Mercier stability in the nonlinear evolution of the interchange mode is studied in the inward-shifted LHD plasma. The beta increase effect is incorporated by employing the multi-scale numerical scheme. The plasma is Mercier unstable in a wide region if there is no deformation of the pressure profile. However, the nonlinear saturation of the interchange mode locally improves the Mercier stability around the resonant surface through the generation of the local flat structure in the pressure profile.

The absolute value of D_I in the stabilized region depends on the pressure increment profile. If we use the similar increment profile, the absolute value of negative D_I becomes much larger in the vicinity of the axis than that in the outer region. This is attributed to that the locally flat structure in the pressure profile is maintained in the beta increase. On the other hand, if we use a parabolic increment profile, the reduction of the pressure gradient is compensated by the increment pressure. Therefore, the absolute values of D_I at all resonant surfaces are in a small level. In the case of the parabola-squared increment profile, the improvement of the Mercier stability extends to the outer rational surfaces. Even in this case, the absolute values of D_I are also limited in a small level including the outer rational surfaces. The level is almost the same as that in the parabolic increment case. These results indicates that the enhancement and the reduction of the pressure gradient is balanced so as to give a critical pressure gradient. The former is due to adding the increment pressure and the latter is due to the nonlinear saturation of the mode. In other words, in the case of the fixed profile of the pressure increment, the plasma is self-organized so that the pressure profile approaches to the marginally stable profile at the resonant surfaces with respect to the Mercier stability.

As a future plan, we consider to include an effect of the equilibrium diffusion. In this case, we can expect that the positive D_I values in the regions between the resonant surfaces also approach to marginal value.

Acknowledgments

This work is supported by NIFS cooperation programs NIFS07KLDD012 and NIFS07KNXN092. and also partly supported by the Grant-in-Aid for Scientific Research (C) 17560736 of the Japan Society for the Promotion of Science.

References

[1] K. Y. Watanabe, et al., Proc. of this conference, I-13 (2007).
[2] K. Ichiguchi, et al., Nucl. Fusion **43**, 1101-1109 (2003).
[3] K. Ichiguchi, et al., Fusion Science and Technology **46**, 34-43 (2004).
[4] K. Ichiguchi B. A. Carreras, J. Plasma Phys. **72** (2006) 1117-1121.
[5] Hirshman, S. P., et al., Comput. Phys. Commun. **43**, 143-155 (1986).
[6] A. H. Glasser, J. M. Greene, J. L. Johnson, Phys. Fluids **18**, 875-888 (1975).